Journal of Southeast University (English Edition) Vol. 25, No. 3, pp. 330 – 334 Sept. 2009 ISSN 1003—7985

Computer aided stitching approach for dental restoration models

Yuan Tianran Dai Ning Cheng Xiaosheng Liao Wenhe

(College of Mechanical and Electrical Engineering, Nanjing University of Aeronautics and Astronautics, Nanjing 210016, China)

Abstract: According to the bio-characteristics of the lower and upper cavity surfaces of dental restoration, a stitching approach is proposed based on a virtual zipper working mechanism and a minimization of the surface total curvature energy, which is used to resolve the stitching problems existing during computer-aided design for dental restorations. First, the two boundaries corresponding to the lower and upper surfaces are triangulated based on the zipper working mechanism to generate the initial stitching surface patch, of which the edges are distributed uniformly between the boundaries. Secondly, the initial stitching surface patch is subdivided and deformed to reconstruct an optimized surface patch according to the bio-characteristics of the teeth. The optimized surface patch is minimally distinguishable from the surrounding mesh in smoothness and density, and it can stitch the upper and lower cavity surfaces naturally. The experimental results show that the dental restorations obtained by the proposed method can satisfy both the shape aesthetic and the fitting accuracy, and meet the requirements of clinical oral medicine.

Key words: dental restoration; model stitching; subdivision and deformation; virtual zipper

The inlay and crown restorations in dental prosthesis are used to restore the shape and function of the teeth, which are damaged or affected by tooth defects, such as caries, malformation, cracks and hypodontia. The traditional restorations making method is a time consuming and labor-intensive work. The patients have to experience wear-reworking many times before achieving a restoration with satisfactory fitting accuracy. With the development of computer technology, the 3D dental model can be easily obtained via different kinds of intra- or extra-oral measurement methods[1-2]. CAD/CAM has been introduced to dentistry discipline and great success has been achieved in clinical applications of orthodontics as well as oral and maxillofacial surgeries[3-6]. The CAD/CAM dental system has simplified the procedures of the restoration production process through digitizing, computer aided design and virtual wearing, and manufacturing. The designing process for inlay and crown restorations are divided approximately into five steps[7]: 1) Prepare and digitize the tooth model; 2) Detect the feature line of the inlay or crown preparation; 3) Extract the lower cavity surface of the inlay or crown restoration using the feature line; 4) Reconstruct the occlusal surface which corresponds to the missing part of the tooth, and then locate and cut to extract the upper cavity surface of the restoration; 5) Stitch the upper and lower cavity surface to obtain a surface patch, which makes the cavity of the restoration watertight. Fig. 1 sketches the typical process of the computer aided design for inlay, which is also adaptable to crown.

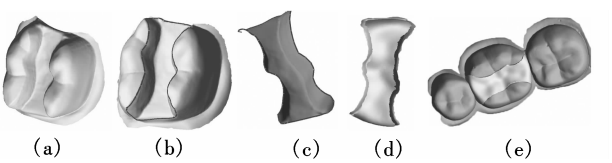

Fig. 1 Illustration of the computer aided inlay restoration design. (a) 3D inlay preparation; (b) Feature line detecting; (c) The lower cavity surface; (d) The upper cavity surface after being located; (e) Inlay restoration and its corresponding virtual wear

In graphics, the efforts in surfaces stitching techniques can be approximately classified into three major categories, namely subdivision[8], implicit[9] and parametric surfaces[10]. The subdivision schemes[8] need given boundary curves, cross-boundary derivatives and initial control nets. Because it is difficult to accurately solve the boundary derivatives for discrete surfaces, it becomes difficult to perform the stitching operation between the triangular meshes using the subdivision schemes. The implicit surface-based stitching method[9] mostly uses volumetric techniques and radial basis functions for surface interpolation to reconstruct the stitching surface. The stitching result is globally optimized, and cannot reflect the local characteristics. The parametric surface-based method[10] uses constraints such as control points and shape influencing tangent magnitudes to construct a virtual stitching surface first, and then obtains the final triangular stitching surface through mapping or re-sampling techniques. The parametric-based stitching method changes the connect relationship of the original surface, which makes the stitching surface seem unnatural.

Because the boundaries corresponding to the upper and lower cavity surfaces are long and with sharp bending changes, it is difficult to obtain a stitching patch which can satisfy both the shape aesthetic and the fitting accuracy by using the existing methods. The stitching results of the upper and lower surfaces have a great influence on whether the restoration can be used in clinical application successfully or not. In this paper, according to the bio-characteristics of the lower and upper cavity surfaces, we propose a stitching algorithm based on a zipper working mechanism and a minimizing total curvature function of the surface patch, which can reconstruct a surface patch satisfying the natural attributes of the tooth.

1 Virtual Zipper and Stitching Algorithm

While the zipper is being closed, the three neighboring teeth of the zipper in contact with each other form the shape

Received 2009-02-20.

Biographies: Yuan Tianran(1982—), male, graduate; Dai Ning(corresponding author), male, associate professor, dai_ning@nuaa.edu.cn.

Foundation items: The National High Technology Research and Development Program of China(863 Program)(No. 2005AA420240), the Key Science and Technology Program of Jiangsu Province (No. BE2005014).

Citation: Yuan Tianran, Dai Ning, Cheng Xiaosheng, et al. Computer aided stitching approach for dental restoration models [J]. Journal of Southeast University (English Edition), 2009, 25(3): 330 – 334.

of a triangle. Because the boundaries of the lower and upper cavity surfaces are near to each other in spatial location. Similar in shape, with nearly equal lengths and number of vertices, each boundary can be seen as a virtual circular zipper with the vertices as the "teeth". The "teeth" contact information of the virtual zipper is represented by a line segment, whose ends are the boundary vertices. Three neighboring line segments connected with each other consecutively at the end form a triangle. Based on the above assumptions, we can imitate the zipper working mechanism to zip the upper and lower cavity surfaces. The difference between the real and virtual zipper used in stitching the surface is that the "teeth" of the virtual zipper can be in contact with more than two "teeth" simultaneously, and remain so during the close operation.

The triangles in the stitching patch obtained above are just connections between the boundary vertices, and have to be subdivided and deformed to obtain an optimized surface patch. It can reflect the local characteristics of the corresponding tooth part and satisfy the fitting accuracy, and it is minimally distinguishable from the surrounding mesh in smoothness and density. Because the surface of a healthy tooth model is curvature continuous, we use the boundary curvature information as a constraint to construct an optimized surface patch, which minimizes the total curvature energy. The following steps describe the procedure of the stitching algorithm:

1) Zip the upper and lower cavity surface along the boundaries to generate the initial stitching surface patch;

2) Subdivide and deform the initial stitching surface patch according to the boundary information in order to obtain a surface patch which can match the density and smoothness of the surrounding mesh.

1.1 Definitions

The 3D dental model is represented by using a watertight or two-manifold triangular mesh. Let M be a two-manifold triangular mesh corresponding to surface S embedded in $\mathbf{R}^3$, and $V = \{v_1, v_2, \ldots, v_n\}$ denotes the set of vertices in M. We define $\mathrm{NV}_1(i)$ as one-ring neighbors of vertex v_i and $\mathrm{NT}_1(i)$ as the set of triangles that share vertex v_i. The boundary edge is an edge that only connects to one triangle, and a boundary vertex is a vertex that is adjacent to a boundary edge. A boundary of the mesh is a closed loop of boundary edges. Let v_i^b represent the boundary vertex. The boundary is denoted by the sequence of vertices $B = \{v_1^b, v_2^b, \ldots, v_n^b\}$.

1.2 Generation of the initial stitching patch

1.2.1 Initialization of the virtual zipper

Let mesh_1 and mesh_2 denote the two meshes corresponding to the upper and lower cavity surfaces to be stitched. B^1_{stitch} and B^2_{stitch} are the corresponding stitching boundaries as shown in Fig. 2(a) where $B^1_{\mathrm{stitch}} = \{v_1^{b_1}, v_2^{b_1}, \ldots, v_m^{b_1}\}$ and $B^2_{\mathrm{stitch}} = \{v_1^{b_2}, v_2^{b_2}, \ldots, v_k^{b_2}\}$. Given vertex $v_i^{b_1}$ on B^1_{stitch}, the closest vertex $v_j^{b_2}$ on B^2_{stitch} is considered as the other end of the "bridge" $v_i^{b_1}v_j^{b_2}$. The boundaries are bridged as shown in Fig. 2(b). Because the boundaries are circular, we obtain two opposite moving directions marked with arrows in Fig. 2(b) at the same starting location. Fig. 2(c) shows the way of the virtual zipper working and it will add one triangle in its moving direction for each step. After the zipper moves one step from the initial state in Fig. 2(b) to that in Fig. 2(c), we obtain a new closed boundary B_{add} ($B_{\mathrm{add}} = B^1_{\mathrm{stitch}} + B^2_{\mathrm{stitch}}$), and then the zipping procedure can also be seen as the triangulation of B_{add} under the condition that the triangles of the triangulation which are used to close the boundary has to satisfy the following prerequisites:

1) The vertices of the triangle have to comprise three consecutive vertices of B_{add}, and the triangle should be oriented consistently with the facets along the boundaries.

2) Each boundary of B^1_{stitch} and B^2_{stitch} has to own at least one vertex of the triangle, but at most two.

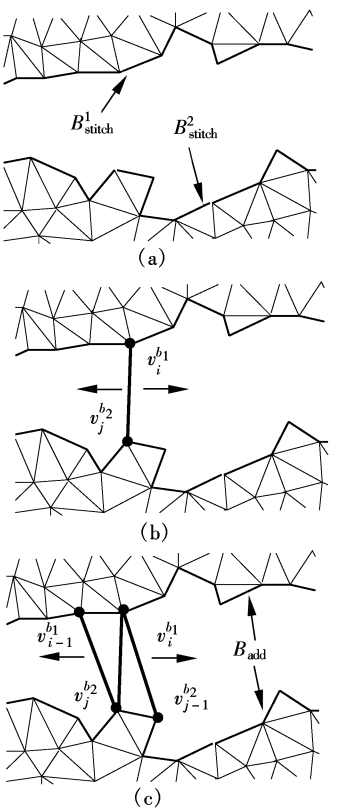

Fig. 2 Mechanism of the virtual zipper. (a) Boundaries to be stitched; (b) The moving direction and location of the virtual zipper; (c) After moving forward one step

1.2.2 Weight rule and zipper closing

When we use the triangulation concept to realize the virtual zipper, we define Ω: $B^3 \rightarrow L$ as the weight function. Here, L is the weight set and Ω assigns a weight for each triangle with three consecutive vertices of B. $|\mathrm{NT}_1(i)|$ denotes the set size of $\mathrm{NT}_1(i)$. Let $\Omega(v_{i-1}^b, v_i^b, v_{i+1}^b)$ be the weight of the triangle $(v_{i-1}^b, v_i^b, v_{i+1}^b)$, and the weight rule is described as follows:

1) If all the three vertices of the triangle $(v_{i-1}^b, v_i^b, v_{i+1}^b)$ belong to B^1_{stitch} or B^2_{stitch} simultaneously, which does not satisfy the prerequisites presented above, the triangle should be given the lowest choice priority: $\Omega(v_{i-1}^b, v_i^b, v_{i+1}^b) = -\infty$.

2) If the triangle $(v_{i-1}^b, v_i^b, v_{i+1}^b)$ satisfies the prerequisites presented above and $|\mathrm{NT}_1(i)| \leqslant 8$, the weight function is computed according to the perimeter l of the triangle. If $|\mathrm{NT}_1(i)| > 8$, the triangle should be added with a higher choice priority in order to obtain an initial stitching patch

with edges uniformly distributed between the boundaries. Then the weight function is

$$\Omega(v_{i-1}^b, v_i^b, v_{i+1}^b) = \begin{cases} -l & |\mathrm{NT}_1(i)| \leqslant 8 \\ \dfrac{|\mathrm{NT}_1(i)|}{8} & |\mathrm{NT}_1(i)| > 8 \end{cases} \quad (1)$$

We apply the following procedure to implement the virtual zipper closing process:

1) Preprocess the boundaries B_{stitch}^1 and B_{stitch}^2 to obtain a new closed boundary B_{add}, and insert the triangles generated to the surface patch M^0 which is initially empty. Compute all the weights according to the weight function given above for each triangle with three consecutive vertices of B_{add}, and insert the weights into L in which the weight is sorted by using an AVL tree.

2) Get the maximum $l_{\max}$ from L and insert its corresponding triangle $(v_{i-1}^b, v_i^b, v_{i+1}^b)$ into M^0. Remove the weights of the triangles $\Omega(v_{i-2}^b, v_{i-1}^b, v_i^b)$, $\Omega(v_{i-1}^b, v_i^b, v_{i+1}^b)$ and $\Omega(v_i^b, v_{i+1}^b, v_{i+2}^b)$ from L that include vertex v_i^b. Eliminate vertex v_i^b from B_{add}, and then $B_H = \{v_1^b, v_2^b, \ldots, v_{i-2}^b, v_{i-1}^b, v_{i+1}^b, v_{i+2}^b, \ldots, v_n^b\}$. Compute the weights $(v_{i-2}^b, v_{i-1}^b, v_{i+1}^b)$, $(v_{i-1}^b, v_{i+1}^b, v_{i+2}^b)$ of the triangles $\Omega(v_{i-2}^b, v_{i-1}^b, v_{i+1}^b)$ and $\Omega(v_{i-2}^b, v_{i-1}^b, v_{i+1}^b)$, and insert them into L. Execute step 2) iteratively until the vertex number of B_{add} is less than three(see Fig. 3(b)).

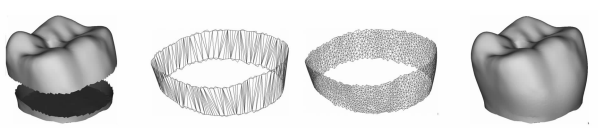

(a) (b) (c) (d)

Fig. 3 Example of the molar tooth model stitching. (a) Model to be stitched; (b) Initial stitching surface patch; (c) After subdivision and deformation; (d) Stitching results

1.3 Subdivision and deformation

The triangles in the initial stitching patch are just the connections between the boundary vertices(see Fig. 3(b)) and have to be subdivided and deformed to obtain an optimized surface patch which can satisfy the fitting accuracy and is minimally distinguishable from the surrounding mesh in smoothness and density. In this paper, the subdivision procedure is performed by adopting the algorithm presented by Pfeifle and Seidel[11] on M^0 to obtain a patch M^1 that approximates the density of the surrounding mesh(see Fig. 3(c)). In computer graphics and the geometry modeling field, the total curvature functional $E(S) = \iint \kappa_1^2 + \kappa_2^2 \, \mathrm{d}A$ is widely used to fair a surface patch with a fixed boundary. Here, κ_1 and κ_2 denote the principal curvatures of the surface, respectively, and $\mathrm{d}A$ is the surface area element. We generalize the fairing method presented by Yoshizawa and Belyaev[12] to deform the surface patch M^1, which is based on the total curvature functional and can produce high quality shapes. The corresponding Euler-Lagrange equation which characterizes the minimizers of $E(S)$ is given by

$$\Delta_S H + 2H(H^2 - K) = 0 \quad (2)$$

where H and K are the mean and Gaussian curvatures, respectively; Δ_S is the Laplace-Beltrami operator. Let $S(u, v, t): \Omega \rightarrow \mathbf{R}^3$ be a family of the smooth surface. u and v are the surface parameters at time t. When the surface family $S(u, v, t)$ evolves along the gradient-descent direction driven by the surface energy, we can solve the following geometry flow to obtain the surface with minimal potential energy given by $E(S)$.

$$\dot{S} = -\nabla E(S) \quad (3)$$

$$\nabla E(S) = -F\boldsymbol{N}, \quad F = -\Delta_S H - 2H(H^2 - K) \quad (4)$$

where $\dot{S}$ is the time derivative of S with respect to t. $\boldsymbol{N}(t, u, v)$ is the unit normal of surface $S(u, v, t)$. To solve (3) numerically, the time derivative term in(3) is approximated by its forward difference approximation

$$\dot{S} \approx \frac{S(t+\tau, u, v) - S(t, u, v)}{\tau} \quad (5)$$

We obtain a discrete surface evolution process by Eqs. (4) and (5),

$$\frac{S(t+\tau, u, v) - S(t, u, v)}{\tau} = -\nabla E(S) \quad (6)$$

$$S(t+\tau, u, v) = S(t, u, v) + \tau F\boldsymbol{N} \quad (7)$$

When Δ_S, H and K are discretized by Meyer et al.[13], the discrete evolution of surfaces (7) can be approximated by a mesh updating process, which is performed iteratively until it reaches a steady-state (see Figs. 3(c) and (d)):

$$v_i^{k+1} = v_i^k + \tau^k F_i^k \boldsymbol{n}_i^k \quad (8)$$

where v_i^{k+1} is the vertex of M^{k+1} obtained after k steps of the updating process (8) from the initial state M^1, which approximates $S(0, u, v)$.

2 Experimental Results and Analysis

The missing parts of the occlusal surface are usually obtained through editing the standard crown, which is stored in the standard crown database, and the feature line of the preparation can be recognized and extracted accurately and efficiently by using existing methods in computer graphics. As can be seen from Fig. 3(b), Fig. 4(b) and Fig. 5(b), the edges of the initial stitching surface patch generated based on the zipper mechanism are distributed between the boundaries evenly, and the weight rule presented above can avoid the situation of self-interference efficiently during triangulation. Fig. 3(c), Fig. 4(c) and Fig. 5(c) show the final results of the stitching surface which match the density and the continuity of the surrounding meshes and the local characteristics of the stitching region can be recovered accurately. The fitting accuracy between the preparation and its corresponding restoration is mostly concerned in clinical application. Because the boundary vertices of the lower cavity surface and the feature line vertices of the preparation are in one-to-one correspondence, the boundary normal information is substituted by the normal information of the feature line in order to make sure that the deformed surface patch can also stitch smoothly across the feature line with the preparation. Because the stitching operation is directly applied on the meshes, and it does not need to be converted into Nurbs or a

B-spline surface, we can reduce the design complexity and improve the accuracy of the contacting region. The virtual wear simulations in Fig. 4(d), Fig. 5(d) and the manufactured object in Fig. 5(e) demonstrate that the algorithm can achieve satisfactory results.

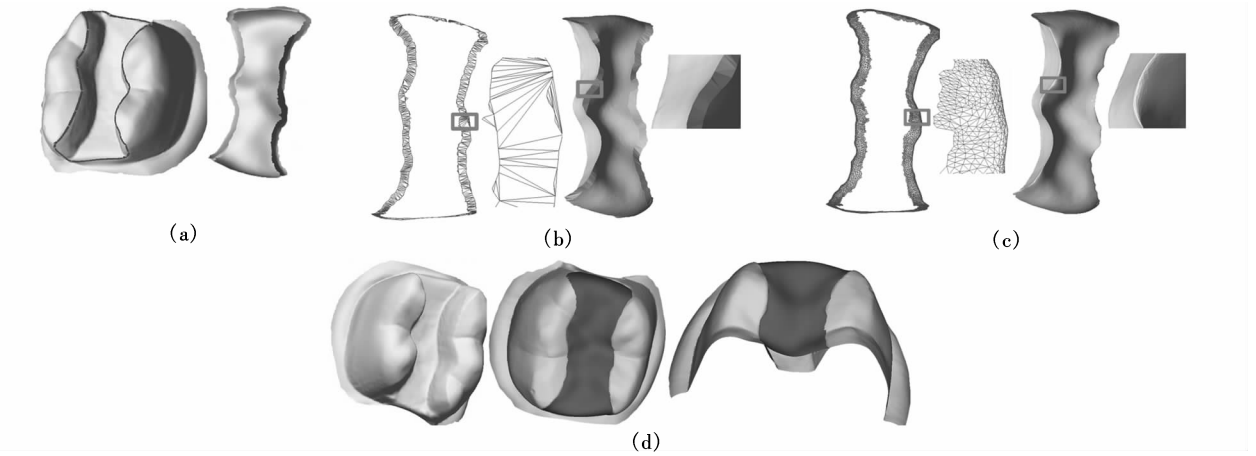

Fig. 4 Stitching process for inlay restoration. (a) Feature line detection, and the corresponding lower and upper cavity surface after being located; (b) The initial stitching surface patch and its corresponding restoration; (c) The surface patch after being subdivided and deformed, and its corresponding restoration; (d) Virtual wear

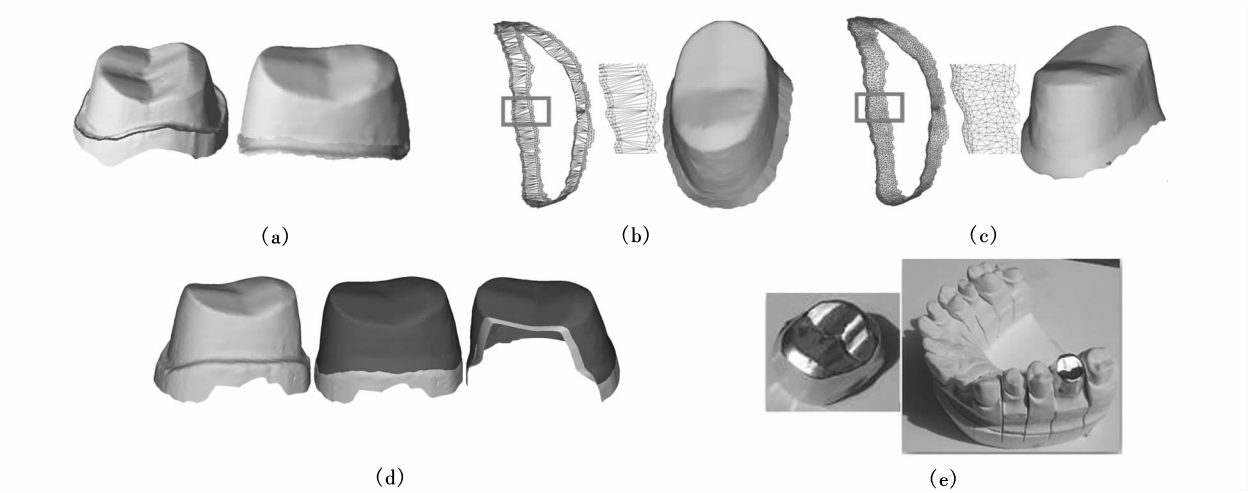

Fig. 5 Stitching process for crown restoration. (a) Feature line detection, and the corresponding lower and upper cavity surface after being located; (b) The initial stitching surface patch with its surrounding triangles, and its corresponding restoration; (c) The surface patch after being subdivided and deformed, and its corresponding restoration; (d) Virtual wear; (e) Manufactured object

3 Conclusion

In this paper, we present a stitching approach to resolve the stitching problems existing during computer aided design for inlays and crowns, such as distortions and fitting inaccuracies. The key of the proposed approach is to reconstruct a surface patch, which can stitch the lower and upper cavity surfaces smoothly and naturally. The experimental results show that the inlay and crown restorations obtained by the proposed method can satisfy the requirements of clinical oral medicine both in virtual wear simulation and in the manufacturing stage. At the same time, the proposed method in this paper is not only restricted to the field of dental restorations, but also it can be used to construct complex objects which share all the features of the original model but differ from the original models in the fields of games, virtual reality, and so on.

References

[1] Hajeer M J, Millett D T, Ayoub A F, et al. Applications of 3D imaging in orthodontics [J]. *Journal of Orthodontics*, 2004, **31**(1): 62 − 70.

[2] Rudolph H, Luthardt R G, Walter M H. Computer-aided analysis of the influence of digitizing and surfacing on the accuracy in dental CAD/CAM technology[J]. *Computers in Biology and Medicine*, 2007, **37**(5): 579 − 587.

[3] Barnfather K D P, Brunton P A. Restoration of the upper dental arch using Lava™ all-ceramic crown and bridgework [J]. *British Dental Journal*, 2007, **202**(12): 731 − 735.

[4] Touchstone A, Phillips R J. Simplifying CAD/CAM Dentistry [EB/OL]. (2005-11-09) [2009-01-10]. http://www.tucsonsmile.com/articles/cad-cam-dentistry.pdf.

[5] Garino F. The orthodontic 3D world: the basic role of the orthodontist [EB/OL]. (2007-08-01) [2009-01-10]. http://www.drgarino.it/pics/upload/Orthotribune.pdf.

[6] Bettega G, Payan Y, Mollard B, et al. A simulator for maxillofacial surgery integrating 3D cephalometry and orthodontia [J]. *Computer Aided Surgery*, 2000, **5**(3): 156 - 165.
[7] Adolph S, Gurke S. Modeling of a fitting inlay from various information[C]//*Proceedings of Vision*, *Modeling*, *and Visualization* 2001. Stuttgart, Germany, 2001: 309 - 316.
[8] Biermann H, Martin I. Cut-and-paste editing of multi-resolution surface [J]. *ACM Transactions on Graphics*, 2002, **21**(3): 330 - 338.
[9] Zou W H, Ding Z, Ye X Z, et al. Interactive point cloud blending by drag-and-drop[J]. *Journal of Zhejiang University*: *Science A*, 2007, **8**(10): 1633 - 1641.
[10] Liu Y S, Zhang H. Mesh blending[J]. *Visual Computer*, 2005, **21**(11): 915 - 927.
[11] Pfeifle R, Seidel H P. Triangular B-splines for stitching and filling of polygonal holes [C]//*Proceedings of Graphics Interface*'96. Toronto, Ontario, Canada, 1996: 186 - 193.
[12] Yoshizawa S, Belyaev A G. Fair triangle mesh generation with discrete elastica [C]//*Proceedings of Geometric Modeling and Processing*. Riken, Saitama, Japan, 2002: 119 - 123.
[13] Meyer M, Desbrun M, Schroder P, et al. Discrete differential geometry operator for triangulated 2-manifolds[C]//*Proceedings of the* 26*th Annual Conference on Computer Graphics and Interactive Techniques*. Los Angeles, USA, 1999: 317 - 324.

计算机辅助口腔修复体模型的缝合算法

袁天然　戴　宁　程筱胜　廖文和

（南京航空航天大学机电学院，南京 210016）

摘要：针对计算机辅助口腔修复体设计中的缝合问题，根据修复体腔底表面和上表面的生物医学特征，提出了一种基于拉链啮合机制和最小化全曲率能量函数的缝合算法. 该算法首先采用由局部最优化权值驱动的虚拟拉链，对修复体腔的底表面和上表面边界进行拉合，得到对应的初始缝合曲面片. 其次，对初始缝合曲面片进行细分优化，并根据牙齿的生理医学特性，对缝合曲面片进行变形调整，构造出符合实际生理医学特征的缝合曲面片，实现修复体腔底表面和上表面的光滑连续缝合. 实验结果表明，利用所提方法设计出的修复体在形态和配合精度上，均能满足临床口腔医学要求.

关键词：口腔修复体；模型缝合；细分变形；虚拟拉链

中图分类号：TP391